

Electronic Structure for C4'-Substituted Stavudine: *ab initio* and DFT Investigation

KARRAR A.S. ALAMEED^{1,*} and FALAH SHAREEF²

¹Department of Chemistry, College of Science, University of Kufa, Najaf, Iraq

²Department of Pharmaceutical Chemistry, College of Pharmacy, University of Kufa, Najaf, Iraq

*Corresponding author: E-mail: karrar.saeed@gmail.com

(Received: 18 February 2013;

Accepted: 23 October 2013)

AJC-14276

In this work, we present the result for electronic structure properties of the stavudine and its 4'-substituents molecules that have involved pseudorotation angle parameters for five sugar member ring, frontal orbital, electrostatic potential maps and total energies, as well as, potential energy surfaces of exocyclic rotation angles at DFT and *ab initio* level theories. Comparisons to D4T and 4'-substituted ones have the major concern of this report. Five sugar member rings of *syn* conformers are more planar corresponding to *anti* ones and the substitution shows a different trends on the two conformations. The substitution at C4' position not cause a significant changes in gap values, whereas, the substitution lead to decrease dihedral angle (χ).

Key Words: DFT, Potential energy surface, Stavudine, Pseudorotation cycle, Puckering.

INTRODUCTION

Human immunodeficiency virus type 1 (HIV-1) uses its own reverse transcriptase (RT) to convert its single stranded RNA genome into a double stranded DNA copy. zidovudine, didanosine, lamivudine (3TC) and stavudine (d4T) are considered the significant class of nucleoside reverse transcriptase inhibitors against HIV-1 infection¹⁻⁴. The modified nucleosides of pyrimidine bases subjected to many studies as potential agent modified nucleosides of pyrimidine bases subjected to many investigations as potential antiviral agents⁵⁻⁹. Unfortunately the clinically applications of these compounds is confined with limits due to their cytotoxicity through inhibition the host DNA polymerase^{9,10} and the rapid emergence of drug-resistant viral mutants. Therefore the studies to physico-chemical properties mad help to understand the behaviour of new classes with reduced cytotoxicity and improved antiviral potency, particularly against drug-resistance viral strains¹¹⁻¹³. Our work employs conventional *ab initio* and DFT calculations to introduce a systematic investigation for D4T and its new novel analogs which are synthesized by Dutschman *et al.*¹⁴ (Fig. 1) shows schematic structures of these molecules.

It's important to know the electronic structure to such flexible systems. The object of this study is to investigate the most electronic structure properties for such important molecules and if there a significant difference in electronic structure properties resulting from substituent on C4' pentofuranosyl position.

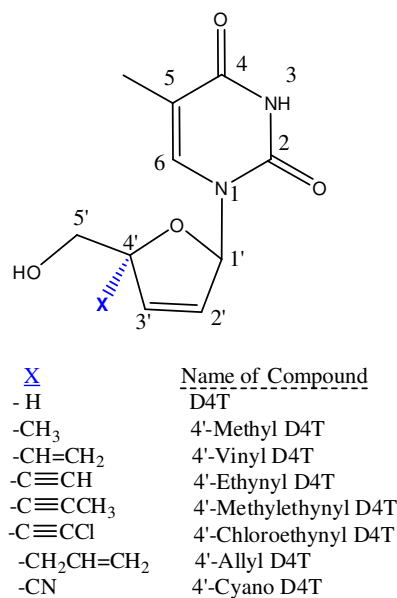


Fig. 1. Structural formula for 4'-substituted D4T

An investigation on the effect of the solvent on the molecular structure and energetics of the most stable conformers of stavudine and thymidine was carried out¹⁵, followed by a study¹⁶ of the tautomerism of this analogs by using the B3LYP and MP2 quantum chemical methods.

The conformation of nucleoside is usually referred by four vital structural parameters^{17,18} the phase angle of pseudorotation

P, describing the puckering of the furanose ring: the north conformer with $-90^\circ \leq P \leq 90^\circ$ and the south conformer with $90^\circ \leq P \leq 270^\circ$, the glycosilic torsion angle χ (*anti* or *syn*), orientation of exocyclic chain above the ring C4'-C5' and orientation of groups attached to pyrimidine moiety. Pseudorotation wheel (Fig. 2) has been used to describe modes of five sugar member ring and pseudorotational phase angle (P) and the maximum puckering amplitude (v_{\max}) are calculated from eqns. 1 and 2.

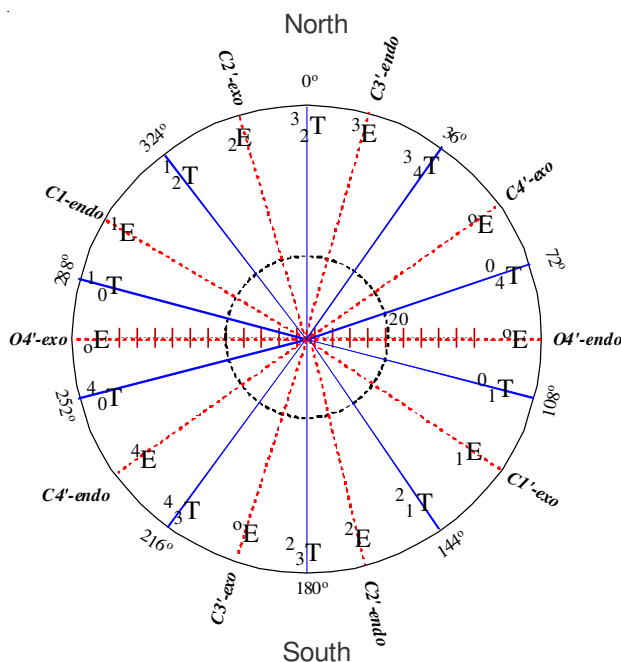


Fig. 2. Pseudorotation wheel for pentofuranosyl nucleosides denotes "twist" and E denotes "envelope". The units of the P and v_{\max} are degrees. The radius of the wheel corresponds to v_{\max} and the small concentric circle encompasses a central region characterized by a flatter sugar moiety ($v_{\max} < 20^\circ$)

Since the arctan function produces angles in the range of -90° to 90° , 180° is added to $\arctan(p)$ when v_2 is negative to obtain the P values in the range of 90° - 270° (south); 360° is added to $\arctan(p)$ in the remaining cases where p is negative to obtain P values in the range of 270° - 360° (north).

$$\tan P = \frac{(v_4 + v_1) - (v_3 + v_0)}{2v_2(\sin 36^\circ + \sin 72^\circ)} \quad (1)$$

$$v_{\max} = \text{obs} \left(\frac{v_2}{\cos P} \right) \quad (2)$$

COMPUTATIONAL METHOD

- Becke three parameter hybrid exchange functionals B3 combined with LYP type correlation Functionals have been employed to find the equilibrium geometry with medium split valence basis sets 6-31G(d) and 6-31G(d,p) using gradient technique without symmetry constrain the calculation results produced two minima *anti* and *syn* conformations with all gradient vectors have exactly zero.

- QST2 mythology, with B3lyp/6-31G(d) and by B3LYP/6311++G(d,p)//B3lyp/6-31G(d) are employed to find the saddle point and to show height of intra-conversion barrier between two *anti* and *syn* conformers .

- Hessian matrix calculated with B3LYP(d) in order to identify the nature of stationary points, there is no any imaginary (negative) frequency onto the stationary points of the two minima, but, one negative eigenvalue of into Hessian matrix is recorded for transition state geometry.

- For accuracy purposes, we use single point calculations in many places. DFT [B3LYP,hybrid functional of Perdew, Burke and Ernzerhof¹⁹ (PBE0)] and *ab initio* [Hartree-Fock, (HF), Møller-Plesset second-order Perturbation theory, (MP2) approximation combined with large Guassian basis sets[6-311+G(d,p), 6-311++G(d,p)], methodologies used to obtain more accurate qualitative energetic results.

- HF method with medium basis set 6-31G(d) used to determine ionization potential according Koopman's theorem, since HF model fully neglecting the electron correlation effects correct the errors of single determinant due to ignoring relaxation of spin orbitals²⁰.

- The pathway for intermolecular conversion from two conformation is employed to confirm the number of stationary points of Potential energy surface, the calculations are current with hybrid Beck method B3LYP/6-31G(d) and single point (sp) energy calculated for each 10 degrees.

- All calculations are carried out using Gaussian03²¹ quantum chemistry package.

RESULTS AND DISCUSSION

Geometrical structure: A geometrical investigation has been carried by evolution pseudorotation phase angle P, maximum amplitude of puckering v_{\max} and the three exocyclic rotation angles χ (O'-C'-N1-C2), γ (C3'-C4'-C5'-O5'), β (H5'-O5'-C5'-C4'). Furanose ring is twisted out of plane in order to minimize non-bonded interactions between their substituents. Table-1 shows P values of *anti* conformers local in range (72-

TABLE-1
PHASE ANGLE, MAXIMUM AMPLITUDE AND TO INTERNAL DIHEDRAL ANGLES γ (O5'-C5'-C4'-C3'), χ (C2-N1-C1'-O1'), β = (H5'-O5'-C5'-C4') OF PUCKERING VALUES IN (DEGREES) EVALUATED BY B3LYP/6-31G(d) LEVEL

N	-X	Anti					Syn				
		P	v_{\max}	γ	χ	β	P	v_{\max}	γ	χ	β
1	-H	92.24	6.46	174.668	-110.45	-53.509	152.64	3.84	176.44	70.915	-59.528
2	-C=CH	90.48	9.52	169.873	-109.43	-51.560	123.77	6.4	171.514	72.067	-57.554
3	-C=C-CH ₃	90.11	9.94	169.624	-109.89	-50.997	121.31	6.52	171.049	72.146	-56.796
4	-C≡N	92.56	9.09	172.784	-108.41	-54.737	128.4	6.32	174.175	70.542	-60.913
5	-C≡C-Cl	90.95	9.89	170.597	-109.67	-52.351	123.25	6.38	172.084	71.897	-58.254
6	-CH=CH ₂	90.29	10.8	167.438	-110.17	-53.656	119.67	7.4	168.845	71.651	-59.364
7	-CH ₂ -CH=CH ₂	87.66	5.85	166.532	-107.74	-53.416	135.01	4.56	167.87	72.563	-59.027
8	-CH ₃	87.24	6.23	168.946	-108.43	-53.268	136.53	4.4	170.542	72.512	-59.246

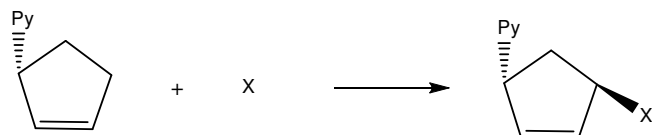
108), in this case the sugar ring take O4'-endo, *i.e.*, *anti* conformers form envelop configuration, in which all atoms of five sugar member ring lying in plane except O4' atom, which prefers to oppositional C5' side, while corresponding *syn* conformers, involving two phase angle modes, one is C2'-exo for D4T and the other, C1'-exo which is obtained by the reminding derivatives has C1'-exo mode. Among other compounds, the largest values of P angles are recorded for *anti* D4T and cyano-D4T conformers.

In other hand, the values of v_{\max} confirm this behaviour. Their results showed irregular variation for the two conformers, the substitution cause increasing in puckering amplitude of five sugar member ring, which is *syn* conformers and the other shows v_{\max} values lower (methyl and allyl)-D4Ts and the larger (the reminding substituents) than D4T.

The substitution of *anti* C4'-position by the different (except cyano) groups in D4T alters the sugar ring conformation from N to S, but that have not showed for *syn* conformer, the furanose rings have (S) type for all *syn* conformers. In general, vinyl substituted D4Ts show larger puckering than other compounds, in addition, the puckering in five sugar member ring of *anti* conformation molecules relatively larger than the corresponding *syn*, overall, the maximum amplitude of puckering is less than 20, that is, the five sugar member ring considerably flat²².

Energetics

Bond dissociation energy (BDE): *Anti*-conformation of this type of inhibitors are necessary for biological activity²³ so we prefer to investigate about strength of C1'-X bond where the different groups link to five member ring of ribose. Table-2 lists bond dissociation energies (BDEs) of nucleoside-group (C1'-X) bond for these different groups for *anti* conformation of D4T and it's derivatives, bond energies vary from model chemistry to another the DFT model different from each other as and each of PBE0 and B3LYP contrast to MP2. "The different approximate solutions to the Schrödinger equation often lead to different predictions. There is no reason why two approximations must give the same trends"²⁴. However, all methods confirm that (C1'-allyl) bond is weaker than the others.



Total and frontal energies: The total energy of two conformations and the difference explicit that *syn* conformation is suffering from more steric than *anti* conformers. In other word the *anti* conformation is energetically preferred than *syn*. This is due to bulky carbonyl group electronic cloud be close over the five sugar member ring. Of course, the correlation energy lower the electronic energies and that reflect on occupies energies, which are derivatives from electronic energy by population analysis, Table-3 agrees with this fact, Hartree common energies for all substituents of both conformations are significantly difference from other level theories, 9.4 eV and unoccupied orbitals in DFT tend to be significantly lower in energy than corresponding HF ones and the highest occupied molecular orbital–lowest unoccupied molecular orbital (HOMO-LUMO) gaps are therefore much smaller with DFT methods than for HF.

In general, KS occupied orbitals are higher than HF orbitals, while virtual KS orbitals are lower than HF orbitals. Therefore, HOMO-LUMO energy gap is larger in HF than in KS.

Ionization energies: Four different level theories are employed to determine Ionization energy according to the fact that negative of HOMOs is representing the energy need to remove their corresponding electrons. (Fig. 3) shows the vertical ionization potentials. HF is logically more give more accurate ionization energies due to two reasons; first because it result derivate for HF theory, the other, although, it is ignore the orbital relaxation, the correlation effect ignoring cancel that error, In general, it's clear that cyanide substituted compounds of two conformers are have higher ionization energy than other substituted compounds.

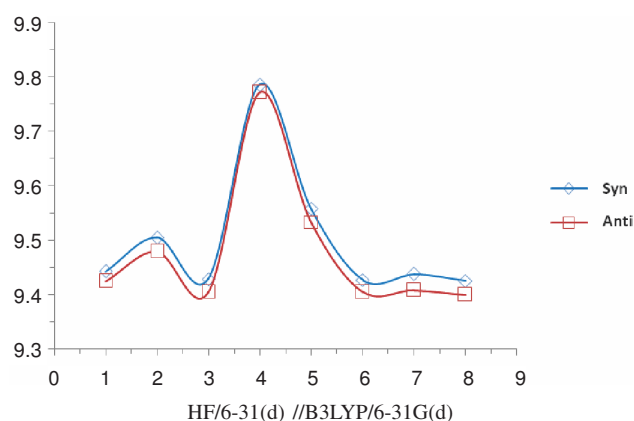


Fig. 3. Vertical ionization potential spectrum according to Koopman's theorem consideration

TABLE-2
BOND DISSOCIATION ENERGIES (BDO) IN Kcal/mol CALCULATED WITH
DIFFERENT MODEL CHEMISTRIES FOR ANTI CONFORMERS IN GROUND STATE

-x	B3LYP/6-31G**	PBE0/6-31G** //B3LYP/6-31G**	MP2/6-31G** //B3LYP/6-31G*
-H	84.3610223	81.0440262	93.0382094
-C≡CH	85.1388361	103.201088	132.048875
-C≡C-CH ₃	84.8622502	102.922112	131.634592
-C≡N	79.5971605	93.9190798	133.222005
-C≡C-Cal	82.1547603	100.583398	72.0912353
-CH=CH ₂	65.2665594	80.0661855	106.232172
-CH ₂ -CH=CH ₂	40.6772572	51.7238847	79.8692218
-CH ₃	59.9476672	74.4973300	91.5437943

TABLE-3
FRONTAL ORBITALS ENERGIES, GAP AND TOTAL ENERGY FOR ANTI AND SYN CONFORMERS

	Anti form				Syn form			
	HOMO (eV)	LUMO (eV)	Gap (eV)	E _{Total} (a.u)	HOMO (eV)	LUMO (eV)	Gap (eV)	E _{Total} (a.u)
-H								
a	-6.55	-1.089	5.462	-798.684528077	-6.563	-1.044	5.519	-798.680878648
b	-6.04	-2.3	3.739	-798.004018930	-5.941	-2.247	3.694	-798.000552138
c	-9.426	2.812	12.238	-794.024169978	-9.443	2.867	12.31	-794.019690693
d	-6.948	-1.641	5.306	-798.925289537	-6.956	-1.598	5.357	-798.921882853
-C≡CH								
a	-6.608	-1.155	5.453	-874.816833806	-6.627	-1.112	5.515	-874.813801768
b	-6.108	-2.375	3.733	-874.063238894	-6.097	-2.315	3.782	-874.060328597
c	-9.480	2.750	12.23	-869.687411116	-9.504	2.807	12.311	-869.683734692
d	-7.271	-1.987	5.284	-875.079149153	-6.979	-1.598	5.381	-875.076393616
-C≡C-CH ₃								
a	-6.523	-1.076	5.447	-914.144310506	-6.536	-1.04438	5.491	-914.140890518
b	-6.009	-2.281	3.728	-913.342471445	-5.961	-2.236	3.726	-913.339113627
c	-9.406	2.820	12.229	-908.733608507	-9.430	2.865	12.294	-908.729415824
d	-6.916	-1.623	5.293	-914.415508063	-6.880	-1.523	5.357	-914.412281757
-C≡N								
a	-6.880	-1.442	5.438	-890.913737069	-6.897	-1.355	5.541	-890.912235663
b	-6.368	-2.656	3.712	-890.157557935	-6.376	-2.549	3.827	-890.156048647
c	-9.773	2.447	12.219	-885.744908195	-9.786	2.553	12.339	-885.743249555
d	-7.271	-1.987	5.284	-891.177340574	-7.282	-1.895	5.387	-891.176134186
-C≡C-Cl								
a	-6.640	-1.192	5.448	-1334.40415034	-6.660	-1.149	5.511	-1334.40133883
b	-6.115	-2.388	3.728	-1333.48491268	-6.104	-2.330	3.774	-1333.48210981
c	-9.534	2.69	12.225	-1328.57655469	-9.559	2.751	12.31	-1328.57320925
d	-7.022	-1.730	5.293	-1334.69140759	-6.996	-1.623	5.373	-1334.68876139
-CH=CH ₂								
a	-6.541	-1.094	5.447	-876.076376906	-6.560	-1.053	5.506	-876.073173490
b	-6.034	-2.309	3.725	-875.3116952	-5.966	-2.254	3.712	-875.308585726
c	-9.405	2.820	0.449	-870.900484826	-9.42664	2.870	12.297	-870.896393199
d	-6.935	-1.643	5.292	-876.337423947	-6.90685	-1.540	5.369	-876.334414131
-CH ₂ -CH=CH ₂								
a	-6.5367	-1.081	5.456	-915.388724744	-6.56235	-1.043	5.519	-915.384769324
b	-6.027	-2.291	3.735	-914.577568153	-5.92696	-2.245	3.682	-914.573659979
c	-9.408	2.822	12.229	-909.932382700	-9.43725	2.872	12.309	-909.927621017
d	-6.932	-1.630	5.302	-915.660361451	-6.90903	-1.531	5.378	-915.656612366
-CH ₃								
a	-6.525	-1.070	5.459	-838.003381695	-6.547	-1.029	5.519	-837.999643446
b	-6.009	-2.276	3.733	-837.275314667	-5.908	-2.225	3.684	-837.271647871
c	-9.400	2.830	12.23	-833.062722083	-9.426	2.884	12.31	-833.058152294
d	-6.876	-1.561	5.315	-838.25358880	-6.932	-1.576	5.357	-838.249991962

a = B3LYP/6-31G(d), b = PBE0/6-311+(d,p)//B3LYP/6-31G(d), c = HF/6-31(d)//B3LYP/6-31G(d) d=B3LYP /6-311++G(d,p)//B3LYP/6-31G(d).

Rotational barrier energies: The activation energy of *anti* and *syn* conformer are obtained for rotation barrier (Table-4), for convert *syn* conformation to *anti* $\Delta E\#1$ for path1 and the corresponding process $\Delta E\#2$ when rotation about single bond is in other side passing over high density Oxygen five member ring atom, $\Delta E\#2$ so, more steric hindrance, so higher barrier value and barrier energy is similar for what is observed experimentally for pyrimidine nucleosides²⁵.

Surfaces

Potential energy surface (PES): The pathway for intermolecular conversion due to rotation about C1'-N1 is described in Figs. 4 and 5, its representation of potential energies surface of relative energy against external rotational angles, a potential curve for 6-31G(d) showing, the comparison of 4-substituted

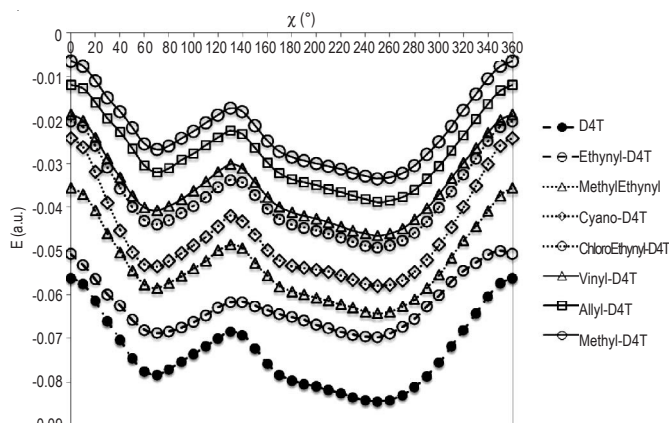


Fig. 4. One dimensional Potential energy surface of external dihedral angle of B3LYP/6-31(d) level theory

TABLE-4
FIRST AND SECOND TRANSITION STATE AND BARRIER HEIGHTS OF TWO CONFORMERS
IN Kcal/mol, REPRESENTED BY B3LYP/6311++G(d,p) // [B3LYP/6-31G(d)] MODEL CHEMISTRY

No.	D4T-X	TS ^a (a.u.)	TS ^b (a.u.)	$\Delta E^{\#c}$ (kcal/mol)	$\Delta E^{\#d}$ (kcal/mol)
1	-H	-798.678154123	-798.919023334	4.000	3.9321
2	-C≡CH	-874.810712941	-875.073247963	3.841	3.7031
3	-C=C-CH ₃	-914.138059660	-914.409414997	3.922	3.8235
4	-C≡N	-890.907284992	-891.170916076	4.049	4.0314
5	-C≡C-Cl	-1334.39807388	-1334.68552846	3.813	3.6892
6	-CH=CH ₂	-876.069945391	-876.331118751	4.036	3.9566
7	-CH ₂ -CH=CH ₂	-915.382445886	-915.654150498	3.94	3.8974
8	-CH ₃	-837.997293248	-838.247666998	3.821	1.458

a = TS energy evaluated by B3LYP/6-31G(d). b = TS energy evaluated by high level theory B3LYP/6311++G(d,p) // RB3LYP/6-31G(d). c = difference between first transition state (TS^a) and total energy of Syn conformer. d = difference between first transition state (TS^b) and total energy of Syn conformer.

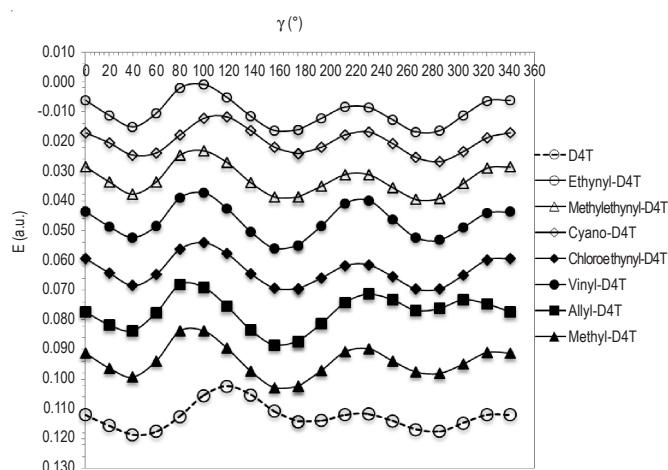


Fig. 5. One dimensional Potential energy surface scheme of γ dihedral angles E total relative energy, (O5'-C5'-C4'-C3')

D4T corresponding to unsubstituted one. The scheme shows that the *anti* conformer is energetically preferred rather than *syn*. In other words, there is no significant change in the χ angle by the substitution, but that effect has shown in the γ exocyclic rotation angle. The D4T curve is different from that of all others. All maxima except cyano-D4T are shifted 20° toward the left side. In other words, the hindered bulky group shows a range (80-100)° rather than (100-120)° of D4T and cyano-D4T. This does not mean that the potential energy surface of D4T matches that of cyano-D4T. The significant difference between the two molecules is shown after the maximum point of the curve. The potential energy surface of D4T is smoother than the substituents behind 160°. Moreover, the allyl-D4T curve shows four peaks, different from all other compounds which have three peaks, due to the bulky non-symmetric allyl group.

It is important to plot the effect of change of two rotation (χ , γ) angles simultaneously with relative energies for D4T (Fig. 6). The important point to notice in this plot is that a drastic change happens in the curve from maxima to minima from 60 to 80 and 340 to 360°, just when the two angles have rotated by 20° at both regions, 60 and 80°, hydrogen bonded. Moreover, the hydrogen bonding between the oxygen of the nitrogen base (O2) and the carboxylic hydrogen (H5'), of the maximum point geometry (1.711 Å) is closer than the corresponding one at the minimum (1.845 Å), but the large cloud of the O5' atom is closer to the minimum point geometry (80°) rather than the maximum one.

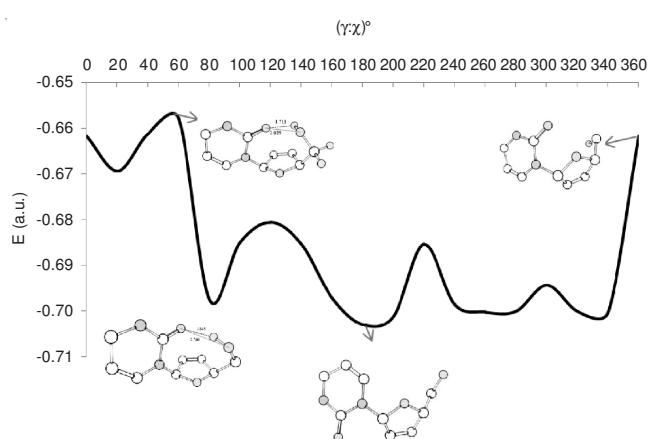


Fig. 6. Potential energy surface: relative energy vs. two rotation angles (γ , χ) of D4T with B3LYP/6-31(d) level theory

Electrostatic potential (EPS): Electrostatic potential representations are illustrated in (Fig. 3) for the *anti* conformer. It is clear that the red area represents the higher electron charge zone and the blue the electron deficient ones. Most of the negative charge concentrates on oxygen and nitrogen atoms in all molecules since these two atoms contain electron pairs. As well as the hydrogen atoms attached to oxygen and nitrogen are suffering from electron density deficiency. It is clear that each Fig. 3a, 3f, 3e compounds have electron density condensed into triple bonds, which is (cyano, ethynyl and methylethynyl)-D4T, whereas the relatively low electron density is on the triple bond with the chloroethynyl substituted compound (Fig. 3h) which does not appear to have bioactivity against NRTIs. Also, the electrostatic potential does not show the cyanostavudine electron density non-localized on the triple cyano group, due to the electron pair on the nitrogen atom.

Conclusion

The results showed that there are four stationary points and one dimensional potential energy surface produced from the pyrimidine ring rotation about the glycosidic bond (N1-C1') with respect to the five sugar ring. The five-membered ring will be less puckered against different substituents. BODs show that allyl substitution is less stable than others. The five-membered ring of the *anti* conformer is more distorted from the *syn*. All substituents in the *syn* conformation cause an increase in the puckering of the sugar ring, but that is not true for the *anti*, the five-membered ring becomes more planar when the allyl and methyl groups have entered.

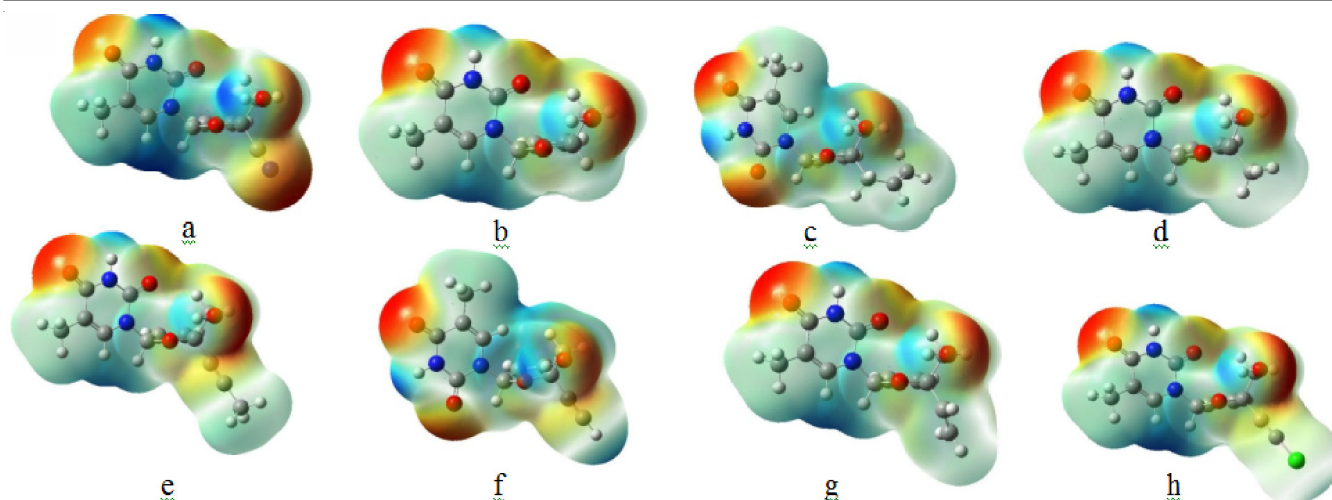


Fig. 7. Total density full SCF matrix electrostatic potential calculated by B3LYP/6-31(d) model chemistry

REFERENCES

1. Y. Amamoto, H. Nakashima, T. Matsui, A. Matsuda, T. Ueda and N. Yamamoto, *Antimicrob. Agents Chemother.*, **31**, 907 (1987).
2. T.S. Lin, R.F. Schinazi, M.S. Chen, E. Kinney-Thomas and W.H. Prusoff, *Biochem. Pharmacol.*, **36**, 311 (1987).
3. T.S. Lin, R.F. Schinazi and W.H. Prusoff, *Biochem. Pharmacol.*, **36**, 2713 (1987).
4. H. Mitsuya, R. Yarchoan and S. Broder, *Science*, **249**, 1533 (1990).
5. N. Dyatkina, A. Arzumanov, A. Krayevsky, B. O'Hara, Y. Gluzman, P. Baron, C. MacLow and B. Polsky, *Nucleosides Nucleotides*, **13**, 325 (1994).
6. G. Andrei, R. Snoeck, J. Balzarini and E. De Clercq, *Nucleosides Nucleotides*, **14**, 559 (1995).
7. C. McGuigan, D. Cahard, H.M. Sheeka, E. De Clercq and J. Balzarini, *Bioorg. Med. Chem. Lett.*, **6**, 1183 (1996).
8. S. Eriksson, B. Kierdaszuk, B. Munch-Petersen, B. Oeberg and N.G. Johansson, *Biochem. Biophys. Res. Commun.*, **176**, 586 (1991).
9. S.N. Rao, *Biophys. J.*, **74**, 3131 (1998).
10. N.A. Foudraire, J.J. de Jong, G.J. Weverling, B.H.B. van Benthem, J. Maas, I.P.M. Keet, S. Jurriaans, M.T.L. Roos, K. Vandermeulen, F. de Wolf and J. Lange, *AIDS*, **12**, 1513 (1998).
11. J. Horwitz, J. Chua, M. Da Rooge, M. Noel and I. Klundt, *J. Org. Chem.*, **31**, 205 (1966).
12. C. Zhu, M. Johansson, J. Permert and A. Karlsson, *J. Biol. Chem.*, **273**, 14707 (1998).
13. E. De Clercq, *Biochem. Pharmacol.*, **47**, 155 (1994).
14. G.E. Dutschman, S.P. Grill, E.A. Gullen, K. Haraguchi, S. Takeda, H. Tanaka, M. Baba and Y.C. Cheng, *Antimicrobiol. Agent. Chem Therp.*, **48**, 1640 (2004).
15. M.A. Palafox, N. Iza, M. de la Fuente and R. Navarro, *J. Phys. Chem. B*, **113**, 2458 (2009).
16. M. Alcolea Palafox and N. Iza, *Phys. Chem. Chem. Phys.*, **28**, 881 (2010).
17. M. Sabio and S. Topiol, *J. Comp. Chem.*, **13**, 478 (1992).
18. V.E. Marquez, A. Ezzitouni, P. Russ, M.A. Siddiqui, H. Ford Jr., R.J. Feldman, H. Mitsuya, C. George and J.J. Barchi Jr., *J. Am. Chem. Soc.*, **120**, 2780 (1998).
19. J.P. Perdew, K. Burke and M. Ernzerhof, *Phys. Rev. Lett.*, **78**, 1396 (1997).
20. A. Szabo and N. Ostlund, *Modern Quantum Chemistry*, Devor Publication Inc, New York, pp. 127-128 (1996).
21. M.J. Frisch, G.W. Trucks, H.B. Schlegel, G.E. Scuseria, M.A. Robb, J.R. Cheeseman, J.A. Montgomery, T. Vreven Jr., K.N. Kudin, J.C. Burant, J.M. Millam, S.S. Iyengar, J. Tomasi, V. Baronem B. Mennucci, M. Cossi, G. Scalmani, N. Rega, G.A. Petersson, H. Nakatsuji, M. Hada, M. Ehara, K. Toyota, R. Fukuda, J. Hasegawa, M. Ishida, T. Nakajima, Y. Honda, O. Kitao, H. Nakai, M. Klene, X. Li, J.E. Knox, H.P. Hratchian, J.B. Cross, C. Adamo, J. Jaramillo, R. Gomperts, R.E. Stratmann, O. Yazyev, A.J. Austin, R. Cammi, C.W. Pomelli, J. Ochterski, P.Y. Ayala, K. Morokuma, G.A. Voth, P. Salvador, J.J. Dannenberg, V.G. Zakrzewski, S. Dapprich, A.D. Daniels, M.C. Strain, O. Farkas, D.K. Malick, A.D. Rabuck, K. Raghavachari, J.B. Foresman, J.V. Ortiz, Q. Cui, A.G. Baboul, S. Clifford, J. Cioslowski, B.B. Stefanov, G. Liu, A. Liashenko, P. Piskorz, I. Komaromi, R.L. Martin, D.J. Fox, T. Keith, M.A. Al-Laham, C.Y. Peng, A. Nanayakkara, M. Challacombe, P.M.W. Gill, B. Johnson, W. Chen, M.W. Wong, C. Gonzalez, J.A. Pople, Gaussian 03, RevisionB.01. Gaussian, Inc., Pittsburgh PA (2003).
22. G. Sun, J.H. Voigt, I.V. Filippov, V.E. Marquez and M.C. Nicklaus, *J. Chem. Inf. Comp. Sci.*, **44**, 1752 (2004).
23. H. Yekeler, *J. Mol. Struct. (Theochem.)*, **684**, 223 (2004).
24. P.M.W. Gill, Personal Communication (2012).
25. D.W. Miles, L.B. Townsend, P. Redington and H. Eyring, *Proc. Nat. Acad. Sci.*, **73**, 2387 (1976).